Available online at www.sciencedirect.com
SCIENCE DIRECT®

Journal of the European Ceramic Society 24 (2004) 855–860

www.elsevier.com/locate/jeurceramsoc

Shear strength and shear failure of layered machinable Ti_3AlC_2 ceramics

Y.W. Bao, J.X. Chen, X.H. Wang, Y.C. Zhou*

Shenyang National Laboratory for Materials Science, High-performance Ceramic Division, Institute of Metal Research, Chinese Academy of Sciences, 72 Wenhua Road, Shenyang, 110016, PR China

Received 10 November 2002; received in revised form 5 April 2003; accepted 21 April 2003

Abstract

Shear-induced failures in uniaxial compression and Hertzian contact damage of Ti_3AlC_2 fabricated by a solid–liquid reaction synthesis were investigated, and shear strength was evaluated using double notched samples and punch hole tests respectively. Compressive strength of 749 MPa and the slip angle of 38° between the slip plane and the loading direction were measured when the applied load was parallel to the hot-pressing direction of the material; whereas the compressive strength of 841 MPa and the angle of 26° were obtained when the applied load was perpendicular to the hot-pressing direction. The shear strength obtained using double-notched sample was 96 MPa and that from punch-shear test was 138 MPa, respectively. SEM fractographs of specimens failed in shear and compression tests indicated a combination of intergranular and transgranular fracture and also an evidence of friction in the slip plane during compression failure process. Punch-shear test was developed and confirmed to be a simple and feasible method for determining the shear strength of layered machinable ceramics.

Keywords: Compressive test; Punch-shear test; Shear strength; Ti_3AlC_2

1. Introduction

The layered ternary ceramic Ti_3AlC_2 is an important number of recently developed "312" families that exhibits unique combination of properties of both metals and ceramics.[1,2] It displays high elastic modulus, low ratio of hardness to modulus and high ratio of fracture toughness to strength K_{IC}/σ_b, metallic electrical conductivity, excellent thermal shock and oxidation resistance, and good machinability.[3–6] Recent works have shown that Ti_3AlC_2 and related ternaries are exceptionally damage tolerant materials and facile machinable. The unique properties of Ti_3AlC_2 are attributed to its crystal and electronic structures.[5] The contribution to the damage tolerance and micro-scale plastic deformation under compressive load consist predominantly of basal-plane slip, delamination and kinking within laminated grains.[1,4,7]

It was noticed that shear-induced failures were the main failure forms of "312" material like Ti_3SiC_2.[7,8] Such a failure mode indicates a low shear resistance in this material, which is responsible for the facile machinability. Knowledge of shear strength and shear-induced failure mechanism in Ti_3AlC_2 is important for safety design and application of this novel ceramic. However, investigation on measuring the shear strength of Ti_3AlC_2 was seldom reported in literature due to difficulties in shear test of ceramics. Although the minimum critical shear stress of 36 MPa in Ti_3SiC_2 (one of "312" materials) has been estimated through measured compressive yield strength (200 MPa) and 65° angle between the loading direction and the slip plane,[9] the critical shear stress in uniaxial compressive test does not equal to the shear strength due to the influence of the compressive stresses normal to the slip plane. Generally, the critical shear stress on the slip plane in compression should be higher than real shear strength, but how much higher depends on the microstructure of the material and the compressive stress normal to the slip plane.

In the present study, shear strength of Ti_3AlC_2 was measured respectively by means of double-notched sample and punch shear tests. Shear failure in compressive

* Corresponding author. Tel.: +86-24-23971762; fax: +86-24-23891320.
E-mail address: yczhou@imr.ac.cn (Y.C. Zhou).

0955-2219/03/$ - see front matter © 2003 Elsevier Ltd. All rights reserved.
doi:10.1016/S0955-2219(03)00328-5

tests in different orientations and contact damage from spherical indentation were also investigated. The objectives of this work were to provide the shear strength of Ti_3AlC_2 and corresponding testing techniques, and to reveal the relationship between real shear strength and the critical shear stress for slip rupture in compression. In addition, a simple method, punch-shear test, was developed for determining the shear strength of machinable ceramics.

2. Experimental

2.1. Shear failure in compressive test

The Ti_3AlC_2 used in this work was prepared with the in-situ hot-pressing/solid–liquid reaction process, which was described elsewhere.[4,6] The mean grain size was about 20–50 μm in diameter and 5–8 μm in thickness. Bending strength and elastic modulus of this material were measured first, using three-point bending method and load-deflection relation, respectively. General mechanical and physical properties are displayed in Table 1. The samples with the size of $2\times2\times4$ mm^3 for compressive tests were cut from the bulk disk. The height of the sample was 4 mm and was parallel to the compressive load. Two groups of specimens (A) loading direction was parallel to the hot pressing direction and (B) loading direction was perpendicular to the hot pressing direction, were tested to investigate the anisotropic behavior of compressive strength and shear slip angle in Ti_3AlC_2. Each group contains four samples. The cross-head rate for the compressive tests was 0.1 mm/min and the average compressive stress corresponding to the shear slip in the sample was taken as the compressive strength. The slip angle between the loading direction and the slip plane was measured using optical microscope after tests. The shear failure planes were observed by scanning electron microscopy (SEM) after compressive tests.

Table 1
Some basic properties of Ti_3AlC_2

Properties	Value	References
Density	4.21 g/cm^3	[1,4]
Coefficient of thermal expansion is	9.0×10^{-6} k^{-1}	[1]
Electrical conductivity	3.48×10^{6} Ω^{-1} m^{-1}	[4]
Vickers hardness	2.7–3.2 GPa	[4]
Young's modulus	270±15 GPa	Present tests
Compressive strength		
load//hot-pressing direction	749±77 MPa	Present tests
load⊥hot-pressing direction	841±40 MPa	
Bending strength	390±11 MPa	Present tests
Shear strength (by punch-shear tests)	138±12 MPa	Present tests
Fracture toughness	7.2 MPa m$^{1/2}$	[4]

In compressive tests, the critical shear stress on the slip plane, τ_α, and the compressive stress normal to the slip plane, σ_α, as shown schematically in Fig. 1, can be calculated based on the elastic mechanics.

$$\tau_\alpha = \sigma \cdot \cos\alpha \cdot \sin\alpha \quad (1)$$

$$\sigma_\alpha = -\sigma\sin^2\alpha \quad (2)$$

where σ is the applied compressive stress and α is the angle between the loading direction and the slip plane. Thus, the critical stresses on the slip plane can be calculated using the measured compressive strength and slip angle.

2.2. Shear strength measured using double-notched sample

The shear strength was measured by using double-notched specimen (DNS) under uniaxial compressive load. The specimens were electrical-discharge machined and the surfaces were diamond-polished; the configuration is schematically shown in Fig. 2. In this work the height h = 20 mm, width W = 7 mm, S = 2 mm and 3 mm thickness were used. The arc shape at both ends of the specimen was designed to avoid unsymmetrical stress in the sample. The crosshead speed in the tests was 0.1 mm/min. It was noticed that if the crack direction was not the same as the symmetric axis, the measured shear strength became much higher, which did not reflect the real shear strength of the material. The measured shear strength usually scattered due to crack deflections. Therefore, the testing data were available only when the crack extended along the symmetric axis. The shear strength τ was calculated by

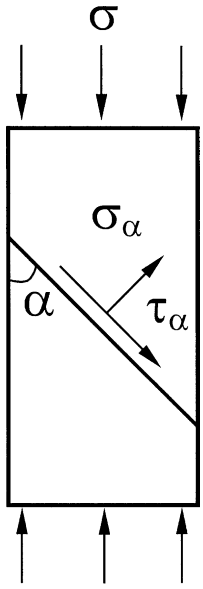

Fig. 1. Schematic of shear slip plane in the sample under uniaxial compressive stress, showing the shear and normal stresses on the slip plane.

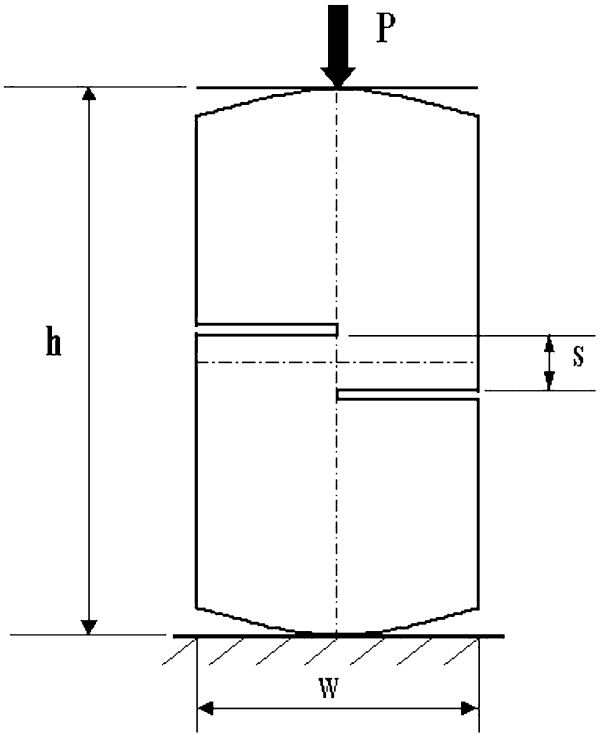

Fig. 2. Schematic of double-notched sample in compressive test for measuring the shear strength.

$$\tau = \frac{P_C}{T \cdot S} \tag{3}$$

where P_C is the critical load, T is the thickness and S is the distance between the notch roots or the length of the fractured face.

2.3. Determining shear strength by punch-shear test

In order to enhance the efficiency and reliability of tests and to simplify sample preparation process for shear tests, a punch-shear test was developed in this study. This simple technique is demonstrated to be valid and convenient for determining the shear strength of the "312" materials. Thin plate specimen with thickness of 0.3–0.4 mm was used for the punch-shear test. There is no strict requirement for the size and shape of the thin plate specimen but the minimum width should be above two times of the diameter of the punch hole. The plate specimen is fixed between two 10 mm thick steel fixtures having a through hole that allows a punch bar with a fit diameter to move through without friction. In this work, the diameter of the punch bar was 2.99 mm and the diameter of the hole was 3 mm, and the loading rate of 0.5 mm/min was applied using universal testing machine. Shear strength τ_f was calculated using the critical load P_c and the shear area.

$$\tau_f = P_c/(\pi dt) \tag{4}$$

where d is the diameter of the punch hole and t is the thickness of the specimen at the punch point. In order to reduce the effects from contact stress in thick specimens, the ratio of sample thickness to diameter of the punch hole, t/d, is required to be ~ 0.1. After the punch test, a small disk will be pushed out from the thin plate specimen and a hole is formed in the specimen. The punched plate sample was observed by optical microscope after the tests.

2.4. Hertzian indentation tests

Hertzian indentations were made using a Si_3N_4 sphere of radius $r = 2.38$ mm at different loads for investigating shear-induced damage in Ti_3AlC_2. The elastic modulus and Poisson's ratio of the indenter were 320 GPa and 0.2, respectively. Bonded-interface specimens were used for observing the sections of the Hertzian contact damage.[11,12] The specimen were prepared by bonding two polished bars of 3 mm×4 mm×30 mm together at a common interface with an intervening thin layer of adhesive, and then polishing the top surface. Indentations were made on the top surface crossing the bonding line, using the cross-head rate of 0.5 mm/min in the tests. Damage zones in the specimens were observed using optical microscope and SEM.

3. Results and discussion

3.1. The critical shear stress in compressive test

It was found that, when the compressive load was parallel to the hot-pressing direction of the material (group A), the slip angle was mostly $\sim 38^\circ$ and the mean compressive strength measured was 749 ± 77 MPa; when the compressive load was perpendicular to the hot-pressing direction of the material (group B), the slip angle was $\sim 26^\circ$ and the mean compressive strength measured was 841 ± 40 MPa. Fig. 3 shows typical profile of shear failure in compressive tests for Ti_3AlC_2 in the two different loading directions. The fractograph Fig. 4 displays the plate layered grains and debris grinded in compression-shearing process that consume more energy than a pure shear failure due to the existence of friction and wear on the slip plane, and the friction was related to grain sizes and the compressive stress normal to the slip plane. Therefore, the critical shear stress τ_α in the slip plane is approximately assumed as the sum of the shear strength τ_f and the friction stress that is related to the compressive stress normal to the slip plane and the friction coefficient.

The mean values of shear and compressive stresses on the slip plane for the two groups of samples were obtained based on Eqs. (1) and (2) from the measured compressive strength and the slip angle.

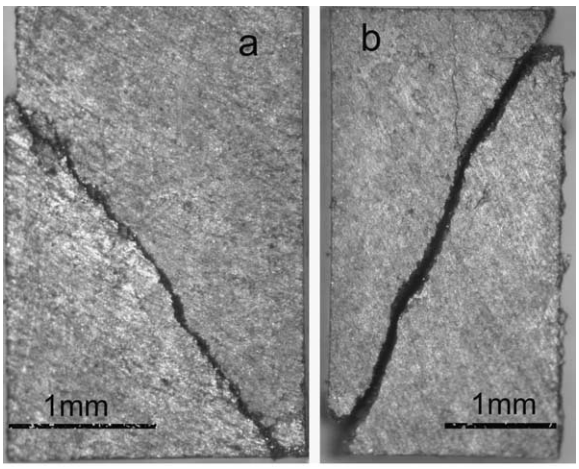

Fig. 3. Failed Ti_3AlC_2 samples ($2\times2\times4$ mm^3) in uniaxial compression tests at two different orientations. (a) The compressive load is parallel to the hot-pressing direction of the material, $\alpha=38^\circ$; (b) The compressive load is perpendicular to the hot-pressing direction, $\alpha=26^\circ$.

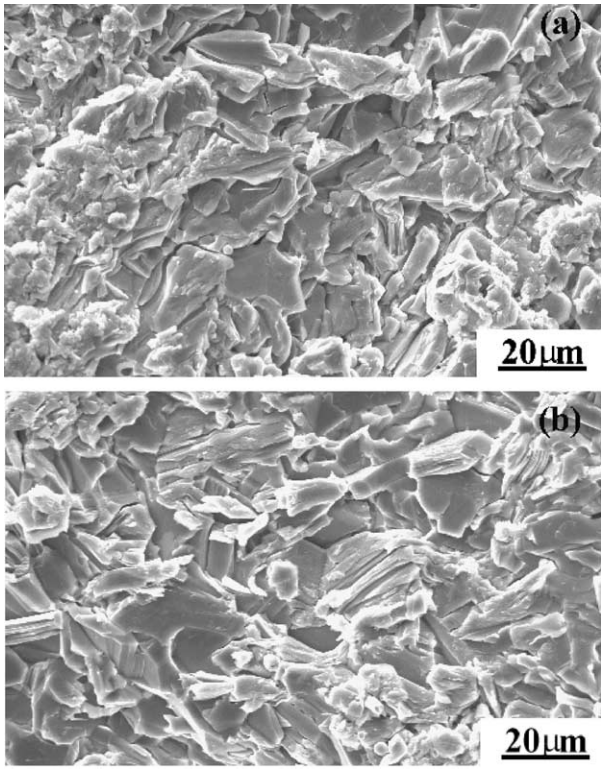

Fig. 4. SEM micrographs of shear slip section in uniaxial compression, showing the plate layered grains and debris grinded in compression-shearing process. (a) Compressive load is parallel to the hot-pressing direction; $\alpha=38^\circ$. (b) Compressive load is perpendicular to the hot-pressing direction, $\alpha=26^\circ$.

Group A: $\sigma=749\pm77$ MPa and $\alpha=38^\circ$, hence $\tau_\alpha=363\pm37$ MPa and $\sigma_\alpha=284$ MPa;
Group B: $\sigma=841\pm40$ MPa and $\alpha=26^\circ$, hence $\tau_\alpha=331\pm16$ MPa and $\sigma_\alpha=161$ MPa;

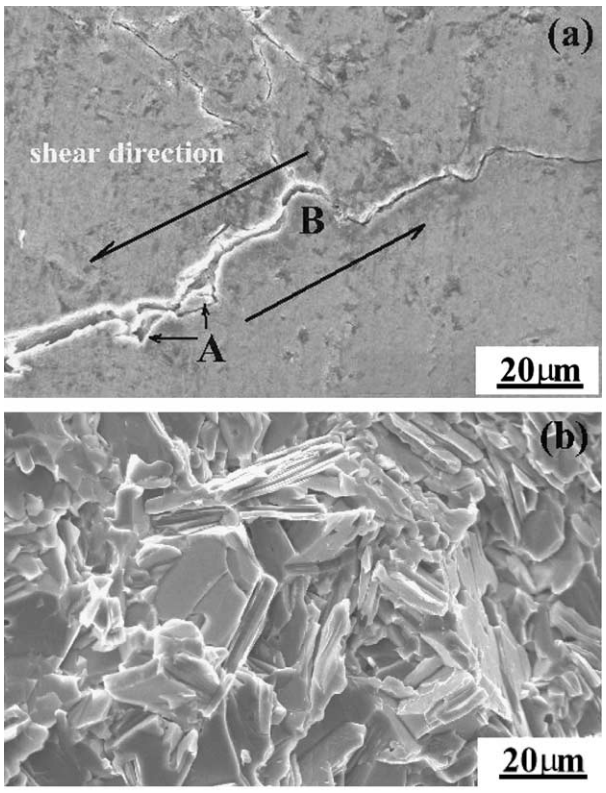

Fig. 5. (a) SEM micrograph of shear-induced crack in double-notched sample, showing the contributions of large grains crossing the slip plane to the shear resistance; (b) the shear-fractured section showing a combination of transgranular and intergranular fracture.

The difference between the measured strength in the two directions was due to the anisotropic microstructure of this layered ceramic. Although qualitative relation between shear strength and the critical shear stress in compressive test was known, determining the shear strength accurately using compressive test was difficult because the friction coefficient was unknown. For Ti_3AlC_2 used in this study, the critical shear stress obtained in compressive tests was about three times of real shear strength.

3.2. Shear strength measured using DNS

Average shear strength in six specimens, 96 ± 22 MPa, was obtained in the tests using double-notched samples. It confirmed that the shear strength was much lower than the critical shear stress in compressive test. The failed samples in this shear test were always integral, not separated into two pieces after unloading, so the shear-induced crack was examined by SEM. The SEM observation indicates that the large grains crossing the slip plane have substantial contribution to shear resistance. Fig. 5a shows the effects of protuberant grains on shear resistance: at point A, two small peaks were pushed down by shear stress; at point B, a relatively large peak

results in a tension-induced crack perpendicular to the main crack at this place. The fractograph Fig. 5b indicates that the shear fracture in Ti_3AlC_2 is a combination of intergranular and transgranular fracture, accompanying delamination in grains and grain comminution caused by friction between the fractured faces. Since the stress concentration near the notch roots was not considered in the calculation in Eq. (3), the shear strength by this method would be a little bit lower than real shear resistance.

3.3. Shear strength measured by punch-shear test

The results obtained from the punch-shear tests show less scatter in the measured shear strength. The punched hole showed perfect shape without crack branching and the shear stress at the boundary of punched disk was considered uniform. The disc and holes in the tested Ti_3AlC_2 sample are displayed in Fig. 6. The mean shear strength of 138 ± 12 MPa was obtained for six punch points at a thin plane sample. The shear strength seems more credible than that from other shear tests because of less influence factors and less scatter in the punch-shear tests. It is $\sim$30% higher than the shear strength obtained form double-notched samples, and is about 1/3 of the bending strength of the same material. By comparing different shear tests, some important advantages of punch-shear test are found, (i) the stability and reliability of testing data is greatly higher than other existing shear methods; (ii) a simple thin plate sample without shape-requirement can produce a set of data. Thus, punch-shear test provides a simple method for determining the shear strength of quasi-plastic ceramics, by which the preparation of samples and loading form become simpler.

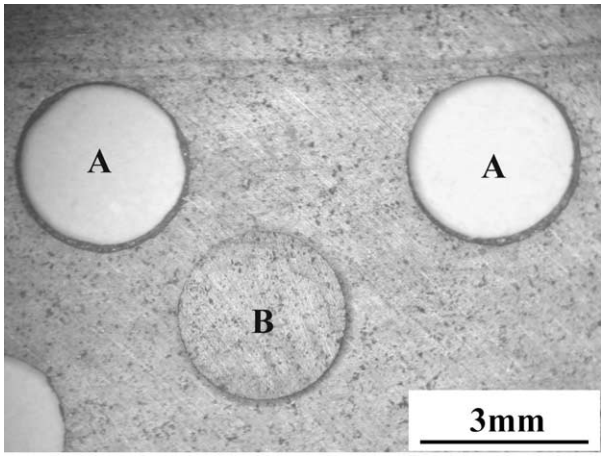

Fig. 6. Profiles of punched specimen and the disc from Ti_3AlC_2 thin plane sample (0.3–0.4 mm thick) after the shear tests; "A" marks the punched hole and "B" marks the disc from the hole. The diameter of the hole was 3 mm.

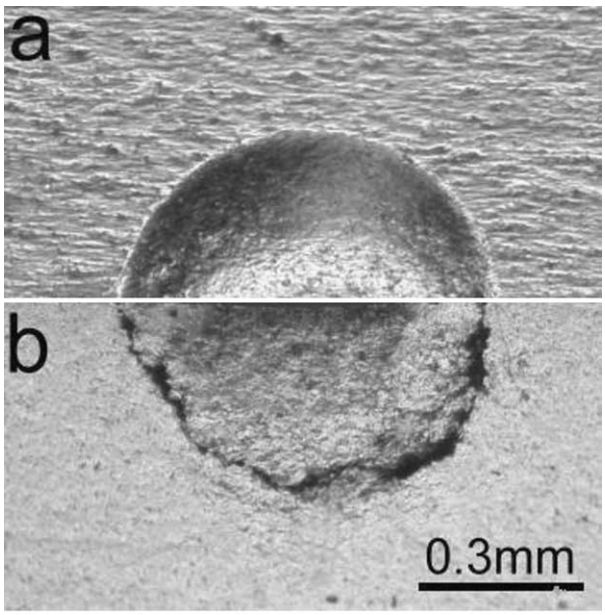

Fig. 7. Optical micrographs of half-surface and side view of contact damage from Si_3N_4 sphere $r = 2.38$ mm at 1.5 kN load, using the bonded specimen.

3.4. Shear-induced damage in Hertzian indentation

Fig. 7 shows the top and side view of the spherical intent on Ti_3AlC_2 sample after Hertzian indentation. Plastic deformation at the contact zone can be observed from the top surface of the indented Ti_3AlC_2 sample. Half-circle crack beneath the indent was found in the cross-section of the indent and the crack shape was almost identical to the trajectory of principal shear stress. At indentation load of 1.5 kN, an apparent boundary was formed which separated the damage zone from the undamaged part of the specimen. Analysis by SEM revealed that the boundary was actually consisted of numerous microcracks and loosened grains. From above tests, it has been demonstrated that the failure mechanism of Ti_3AlC_2 under compressive stress and contact stress was obviously shear-induced failure. For the quasi-brittle material like Ti_3AlC_2, the half-circle cracks around damage zone reflected the shear dependence of failure and a low shear resistance in this ceramic. This feature is very similar to the contact damage in Ti_3SiC_2.[8,10]

The above experimental results indicate that shear strength is the lowest one, compared to the tensile, compressive, and bending strength of Ti_3AlC_2. The low shear strength, and shearing-activated intergranular sliding is the key factor to the exceptional quasi-plasticity of Ti_3AlC_2. The low shear strength is also responsible for the facile machinability of this ceramic. In addition, the low shear strength resulted in the low compressive strength and low hardness, because the

compressive strength of this kind of materials that fracture along shear slip plane under uniaxial compression depends on shear strength.

4. Conclusions

1. Shear slip failure in uniaxial compressive test was confirmed in Ti_3AlC_2. When the loading was parallel to hot-pressing direction of the material, compressive strength of 749 ± 77 MPa and slip angle of $\sim 38^\circ$ were obtained; when the loading was perpendicular to the hot-pressing direction, compressive strength of 841 ± 40 MPa and $\sim 26^\circ$g angle were measured.
2. The average critical shear stress on the slip plane in compressive tests of Ti_3AlC_2 was measured to be ~ 340 MPa, it was much higher than the shear strength, ~ 138 MPa measured by punch shear test and ~ 96 MPa measured by double notched sample. This difference between the critical shear stress and shear strength was imputed to the actions of the compressive stress normal to the slip plane. The shear strength measured by DNS was lower than that measured by punch-shear tests, that was mainly due to DNS involved stress concentration and crack deflection at the roots of both notches.
3. Plastic indent on the surface and half-circle crack along the principal shearing band in the indented Ti_3AlC_2 sample confirmed that the low shear strength and shearing-activated intergranular sliding were the key factors to the exceptional quasi-plasticity of Ti_3AlC_2 and were also responsible for facile machinability and low compressive strength of this ceramic.
4. Punch-shear test, using a ratio of $t/d \approx 0.1$, is a simple and feasible method for measuring shear strength of layered machinable ceramics.

Acknowledgements

This work was supported by the National Outstanding Young Scientist Foundation (No. 50125204 for Y. Bao and No.59925208 for Y. Zhou), National Science Foundation of China under Grant No. 50232040, and "The Hundred-Talent Program" of Chinese Academy of Sciences for Y. Bao and "863" program in China.

References

1. Tzenov, N. V. and Barsoum, M. W., Synthesis and characterization of Ti_3AlC_2. *J. Am. Ceram. Soc.*, 2000, **83**, 825–832.
2. Barsoum, M. W. and El-Raghy, T., Synthesis and characterization of a remarkable ceramic: Ti_3SiC_2. *J. Am. Ceram. Soc.*, 1996, **79**(7), 1953–1956.
3. Wang, X. H. and Zhou, Y. C., Oxidation behavior of Ti_3AlC_2 powders in flowing air. *J. Mater. Chem.*, 2002, **12**(9), 2781–2785.
4. Wang, X. H. and Zhou, Y. C., Microstructure and properties of Ti_3AlC_2 prepared by the solid–liquid reaction synthesis and simultaneous in-situ hot pressing process. *Acta Mater.*, 2002, **50**(12), 3141–3149.
5. Zhou, Y. C. and Wang, X. H., Electronic and structural properties of the layered ternary carbide Ti_3AlC_2. *J. Mater. Chem.*, 2001, **11**, 2335–2339.
6. Wang, X. H. and Zhou, Y. C., Solid-liquid reaction synthesis of layered machinable Ti_3AlC_2 ceramic. *J. Mater. Chem.*, 2002, **12**, 455–460.
7. Zhou, Y. C. and Sun, Z. M., Micro-scale plastic deformation of polycrystalline Ti_3SiC_2 under room-temperature compression. *J. Eur. Ceram. Soc.*, 2001, **21**, 1007–1011.
8. Low, I. M., Lee, S. K., Lawn, B. R. and Barsoum, M. W., Contact damage accumulation in Ti_3SiC_2. *J. Am. Ceram. Soc.*, 1998, **81**(1), 225–228.
9. Barsoum, M. W. and El-Raghy, T., Room-temperature ductile Carbides. *Met. Mater. Trans*, 1999, **30A**, 363.
10. Low, I., Vickers contact damage of micro-layered Ti_3SiC_2. *J. Eur. Ceram. Soc.*, 1998, **18**, 709–713.
11. Guiberteu, F., Padture, N. P. and Lawn, B. R., Effect of grain size on Hertzian contact damage in alumina. *J. Am. Ceram. Soc.*, 1994, **77**(7), 1825–1831.
12. Lawn, B. R., Indentation of ceramics with spheres: a century after Hertz. *J. Am. Ceram. Soc.*, 1998, **81**(8), 1977–1994.